Iron–chromium–carbon–vanadium white cast irons – the microstructure and properties

Mirjana M. Filipović

University of Belgrade, Faculty of Technology and Metallurgy, Belgrade, Serbia

Abstract

The as-cast microstructure of Fe–Cr–C–V white irons consists of M_7C_3 and vanadium rich M_6C_5 carbides in austenitic matrix. Vanadium changed the microstructure parameters of phase present in the structure of these alloys, including volume fraction, size and morphology. The degree of martensitic transformation is also dependent on the content of vanadium in the alloy. The volume fraction of the carbide phase, carbide size and distribution has an important influence on the wear resistance of Fe–Cr–C–V white irons under low-stress abrasion conditions. However, the dynamic fracture toughness of Fe–Cr––C–V irons is mainly determined by the properties of the matrix. The austenite is more effective in this respect than martensite. Since the austenite in these alloys contained very fine $M_{23}C_6$ carbide particles, higher fracture toughness was attributed to a strengthening of the austenite during fracture. Besides, the secondary carbides which precipitate in the matrix regions also influence the abrasion behavior. By increasing the matrix strength through a dispersion hardening effect, the fine secondary carbides can increase the mechanical support of the carbides. Deformation and appropriate strain hardening have occurred in the retained austenite of Fe–Cr–C–V alloys under repeated impact loading. The particles of precipitated $M_{23}C_6$ secondary carbides disturb dislocations movement and contribute to increase the effects of strain hardening in Fe–Cr–C–V white irons.

Keywords: Fe–Cr–C–V white irons, microstructure, hardness, abrasion wear resistance, fracture toughness, repeated impact resistance.

Available online at the Journal website: http://www.ache.org.rs/HI/

REVIEW PAPER

UDC 669.131.2:630.18

Hem. Ind. **68** (4) 413–427 (2014)

doi: 10.2298/HEMIND130615064F

High chromium white cast irons are an important class of wear resistance materials currently used in a variety of applications where stability in an aggressive environment is a principal requirement, including the mining and mineral processing, cement production, slurry pumping and pulp and paper manufacturing industries.

For abrasion resistance, nearly all high chromium cast irons are used as hypoeutectic alloys containing 10–30 wt.% Cr and 2–3.5 wt.% C. The abrasion resistance of these alloys is primarily determined by the features of M_7C_3 carbides, such as their volume fraction [1-6], hardness [1,2], morphology [7,8] and orientation [9–12]. The structure of the matrix that supports the carbides may be extensively altered by alloying and heat treatment [2,3]. It has been already shown that both factors have significant influence on the wear behaviour [1,2,4]. The eutectic carbides play a strong role in influencing the fracture toughness of white irons [1,13–15]. It has been observed that the proportion of eutectic carbides on fracture surfaces is greater than that measured on polished sections [5]. This reflects the brittle nature of the eutectic carbides, with cracks preferentially following the carbide structure. Increasing the carbide volume would increase the number of brittle carbides in the structure, while reducing the amount of matrix material between these carbides. As expected, increased carbide volume decreases the fracture toughness for both austenitic and martensitic matrix [4,13,15].

Extensive industrial applications of high-chromium white cast irons have attracted researchers to try different carbide-forming elements such as tungsten [16,17], niobium [16,18–25], vanadium [16,21,26–34], titanium [19,21,35–39] and boron [40] to further improve this type of material. The addition of an alloying element which confines carbon in the form of a carbide different from cementite, with a greater hardness and more favorable morphology, and which reduces the carbon content of the matrix, allows the simultaneous improvement of both toughness and abrasion resistance [2,21,25,26,29]. By controlling the morphology of the carbide phase and the matrix structure in these materials, significant improvement of toughness and service life may be achieved.

The main goal of adding molybdenum to white cast iron is to improve hardenability. However, only part of the molybdenum contributes to this goal. The presence of carbon in the alloy and its chemical affinity for molybdenum promotes the formation of M_2C or M_6C carbides at the end of the solidification process

Correspondence: Faculty of Technology and Metallurgy, University of Belgrade, Karnegijeva 4, 11120 Belgrade, Serbia.
E-mail: mirjanaf@tmf.bg.ac.rs
Paper received: 15 June, 2013
Paper accepted: 5 September, 2013

[19,41,42]. Addition of the tungsten to high chromium white iron leads to the formation of M_6C carbide (upper than 10% W) that crystallizes in a finely dispersed form as eutectic in the final stage of solidification [16,17]. The introduction of niobium to high chromium white irons resulted in the preferential formation of NbC which is appreciably harder than other carbides present and which forms efficiently since niobium is partitioned fully to these phases [18,19,22,23]. Subsequently, niobium improves the hardness, wear resistance and fracture toughness [20,21,25]. The solubility of titanium to molten cast iron is so small that fine TiC carbides precipitate at higher temperature even in the low titanium-bearing melts, and they likely affect the following solidification [36, 39]. Cerium has limited solubility in austenite and M_7C_3 eutectic carbide [25, 43, 44]. This element formed inclusions in high chromium white irons [45, 46]. In hypoeutectic alloys, around the very fine inclusions of cerium, the carbide particles rich in chromium were formed. The carbide particles can act as the heterogeneous nuclei of austenitic dendrites to enhance nucleation or interfere with their growth and improve the refinement of primary dendrites [45].

Vanadium appeared to be of special interest, due to its double effects, on both the matrix structure and stereological characteristics of carbides. The aim of this paper is to review the microstructural characteristics and properties relevant to the service performance of hypoeutectic Fe–Cr–C–V white cast irons, namely the hardness, abrasion wear resistance, fracture toughness and repeated impact resistance.

MICROSTRUCTURAL DEVELOPMENT

The as-cast microstructure of hypoeutectic F–Cr–C––(V) white irons (chemical composition listed in Table 1) consists of primary austenite dendrites and eutectic colonies composed of M_7C_3 carbides and austenite (Fig. 1).

Also, vanadium rich carbides are found in Fe–Cr–C–V irons containing 1.19–4.73% V (Fig. 2). Vanadium carbide present in these alloys was identified as M_6C_5 type carbide (Fig. 2) and its stoichiometric formula is $V_{3.6}Cr_{1.2}Fe_{1.1}C_5$ [34]. The same type of carbide was found by de Mello *et al.* [28] in cast iron containing 10% Cr and 6% V.

Dupin and Schissler [47] did not detect the vanadium carbide formation in high chromium white cast

Table 1. Chemical composition (mass.%) of Fe–C–Cr–V white irons

Alloy	Element									
	C	P	S	Si	Mn	Mo	Cu	Ni	Cr	V
1	2.89	0.025	0.061	0.85	0.71	0.48	0.99	0.100	19.03	0.0012
2	2.92	0.026	0.063	0.87	0.76	0.45	1.02	0.099	19.01	0.12
3	2.88	0.025	0.061	0.86	0.72	0.42	0.98	0.098	18.89	0.49
4	2.92	0.025	0.061	0.85	0.75	0.43	1.01	0.098	19.04	1.19
5	2.87	0.024	0.063	0.87	0.73	0.44	1.01	0.099	18.92	2.02
6	2.91	0.027	0.061	0.84	0.73	0.44	1.00	0.096	19.05	3.28
7	2.93	0.026	0.062	0.83	0.74	0.43	1.01	0.098	19.07	4.73

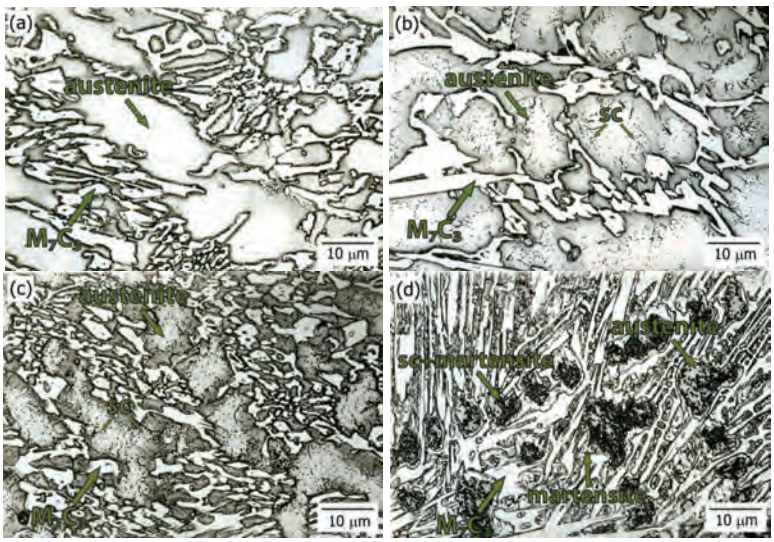

Fig. 1. Optical micrographs of hypoeutectic Fe–Cr–C–V white iron containing: a) 0.12% V, b) 0.49% V, c) 1.19% V, d) 3.28%V.

iron with 1% V. Nonetheless, Bedolla-Jacuinde [21] in 16.9% Cr–2.58% C–1.98% V alloy and Matsubara *et al*. [48] in 17.54% Cr–3.57% C–3.14% V alloy observed that (γ + MC) eutectic solidification did not occur because of lower vanadium content, which was different from the report of Stefanescu and Cracium [49] who indicated that vanadium carbides are present in the microstructure of 14.66% Cr–2.95% C–2.9% V alloy. Furthermore, Sawamoto *et al.* [16] found that vanadium carbides formed in high chromium white cast irons contained more than 5% V. The established disagreement appears to be a result of different cooling conditions, on one hand, and of the fact that vanadium carbides are difficult to notice due to their small volume fraction and size, on the other hand.

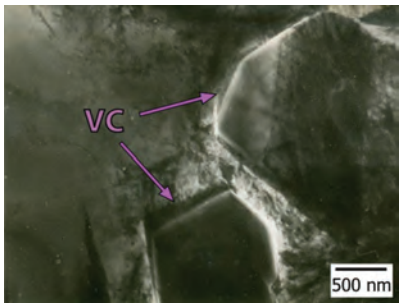

Fig. 2. TEM Micrograph of the Fe–Cr–C–V white iron containing 1.19% V showing vanadium carbide.

Solidification behaviour

With an increase of vanadium content, the alloy composition approaches the eutectic composition in quaternary Fe–Cr–C–V system, causing a decrease of the solidification temperature interval (Table 2).

Solidification starts with formation of *γ*-phase at 1341 °C in Fe-Cr-C alloy with no vanadium addition, at 1319 °C in Fe–Cr–C–V alloy containing 1.19% V, and at 1284 °C in Fe–Cr–C–V alloy containing 4.73% V. In the course of primary γ-phase growth, the composition of the remained liquid was changing. Due to limited solubility of carbon, chromium and vanadium in the austenite, these elements accumulated in front of the progressing solid-liquid interface. At temperatures little bit lower than *liquidus* temperature (1315 °C in alloy containing 1.19% V, 1278 °C in alloy containing 4.73% V) during the eutectic reaction that takes place, in local areas enriched in vanadium, eutectic composed of vanadium rich carbide and austenite was developed. The particles of vanadium carbides disturb or completely block further *γ*-phase growth, with the efficiency depending on their volume fraction, size and distribution [34].

As the temperature falls and solidification progresses, primary austenite dendrites reject solute (carbon, chromium and vanadium) in to the remaining liquid until the eutectic composition is reached and the monovariant eutectic reaction ($L \rightarrow \gamma + M_7C_3$) takes place. From the melt remained in interdendritic regions the coupled austenite–M_7C_3 eutectic was forming at 1244 °C in Fe–Cr–C alloy with no vanadium addition, at 1249 °C in alloy containing 1.19% vanadium, and at 1257 °C in alloy containing 4.73% vanadium. Bedolla-Jacuinde *et al*. [50] found that M_7C_3 eutectic carbides in high chromium white irons nucleated on the surface of the primary and secondary dendrites arms. The eutectic *γ*-phase nucleated side-by-side with the hexagonal M_7C_3 carbides, and both eutectic constituents may then grow more or less at the same rate with bars surrounded by austenite, and coupled growth develops.

The eutectic regions of carbide and austenite grow as colonies, indicating growth of a faceted–non-faceted eutectic [27,51]. Irregular eutectic structures are developed when a non-faceted phase is coupled with a faceted phase. In such eutectics, local morphological adjustment of interphase spacing is severely encumbered by the limited branching ability of the highly anisotropic faceted phase containing planar defects. Thus, the spatially non-uniform or irregular structure that evolves during faceted–non-faceted eutectic solidification is inherently three-dimensional, where the relationship between the growth mechanisms of the faceted phase and the complex non-isothermal interface structure gives rise to a more diverse range of solidification microstructures than that exhibited by regular eutectics [27,51,52]. It has been reported [52] that solute elements, even in trace amounts, may have a strong influence on eutectic growth morphology.

Table 2. DTA Results of the Fe–Cr–C–V white irons during cooling at a rate of 5 °C min^{-1}

Alloy	V in alloy, mass%	Temperature, °C			
		T_L	$T_{E_1(V_6C_5+\gamma)}$	$T_{E(M_7C_3+\gamma)}$	ΔT
1	–	1341	–	1244	97
4	1.19	1319	1315	1249	70
5	2.02	1310	1306	1251	59
6	3.28	1299	1294	1254	45
7	4.73	1284	1278	1257	27

T_L – the start temperature of the austenite reaction (liquidus); $T_{E_1(V_6C_5+\gamma)}$ – the temperature of the eutectic reaction $E_1(L \rightarrow V_6C_5+\gamma)$; $T_{E(M_7C_3+\gamma)}$ – the temperature of the eutectic reaction $E(L \rightarrow M_7C_3+\gamma)$; ΔT – the solidification temperature interval

With increasing vanadium content in the alloy, the volume fraction of primary austenite is decreased, whereas the amount of M_7C_3 and M_6C_5 carbides are increased. In addition, dendrite arms spacing (DAS) and size of eutectic M_7C_3 carbides are decreased, while the size of M_6C_5 carbides is increased with increasing vanadium content (Table 3). When the solidification temperature interval is narrower (as the consequence, in this case, of alloying high chromium white iron with vanadium), around the primary dendrite of the *γ*-phase in the remaining portion of the melt, the temperature and concentration conditions appear more readily, thus enabling the formation of eutectic colony nuclei and their growth which results in the interpretation of further *γ*-phase growth [34]. The eutectic colonies growth rate is well increased with increasing eutectic temperature, *i.e.*, with a lowering of the solidification temperature interval, thus influencing the formation of a larger amount of finer M_7C_3 carbides (Table 3).

Morphology of M_7C_3 eutectic carbide

M_7C_3 carbide has a pseudo-hexagonal structure with lattice parameters a = 13.9820 Å and C = 4.5065 Å, point group *mmm* and space group *Pmna* [53]. M_7C_3 forms as eutectic carbide during solidification with a distinguishable characteristic that it always appears to contain a high concentration of structural faulting [2]. Figure 3 shows a part of the eutectic M_7C_3 carbide containing many twins.

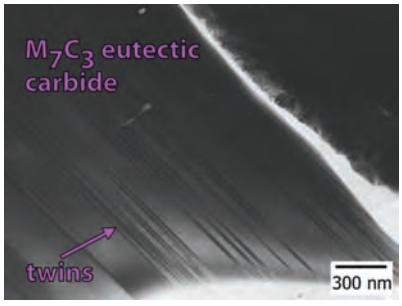

Fig. 3. TEM Micrograph of Fe–Cr–C–V white iron containing 1.19% V showing hexagonal M_7C_3 eutectic carbide.

The SEM micrographs of deep etched sample revealed that single M_7C_3 eutectic carbides in white iron, were rod or blade shaped, where the blades are basically consist of multiple rods (Fig. 4). The hexagonal $(Cr,Fe)_7C_3$ carbides grow as rods and blades, with the fastest [1] growth direction, and form a continuous network within each eutectic colony [9].

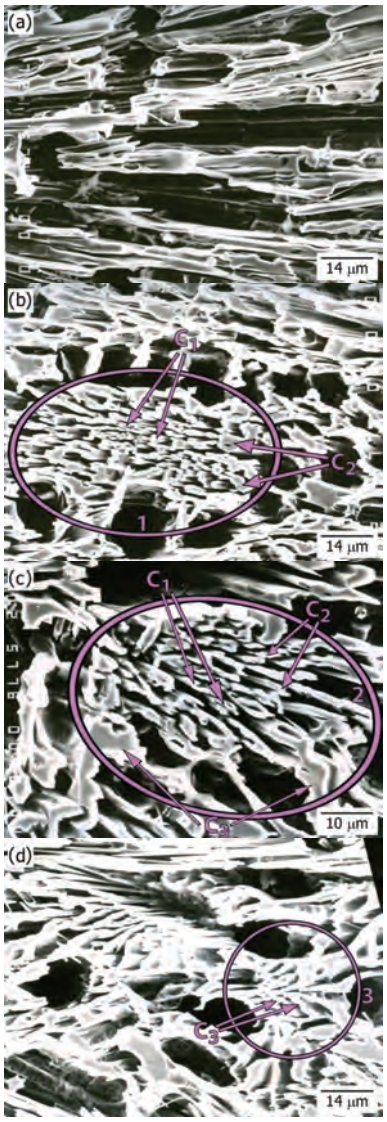

Fig. 4. SEM Micrographs of deep etched sample showing morphology of M_7C_3 eutectic carbides in hypoeutectic Fe–Cr–C–V type alloy containing 1.19% V. Different morphologies of eutectic colonies are marked 1 to 3. M_7C_3 carbides of different compositions marked by arrows C_1 to C_3.

Table 3. The volume fraction and size of phases in the microstructure of Fe–Cr–C–V white irons

Alloy	V in alloy, mass%	Volume fraction, vol.%			Size, μm		
		Primary γ-Fe	M_7C_3	M_6C_5	DAS	M_7C_3	M_6C_5
1	–	50.83	30.97	–	14.08	7.48	–
4	1.19	47.48	31.96	1.58	12.76	6.74	1.26
5	2.02	45.76	32.82	2.31	11.93	6.52	1.31
6	3.28	42.05	34.31	3.12	10.67	5.67	1.45
7	4.73	39.15	35.47	4.27	9.45	5.03	1.52

In the Fe–Cr–C–(V) type alloys, three different compositions of M_7C_3 carbides with different the Fe/Cr ratio of atomic fraction have been found (Table 4). While Fe/Cr ratio of atomic fraction in Fe–Cr–C–V alloy containing 0.12% V is 0.71 for carbides of composition C_1, it is 0.99 for carbides C_2 and 1.31 for carbides of composition C_3. In C_1 and C_2 carbides of the alloy containing 1.19% V, vanadium substitutes chromium atoms in M_7C_3 carbides lattice, while in carbide of composition C_3, it substitutes iron atoms. The Fe/Cr ratio in this alloy is 0.79, 1.03 and 1.26 for carbides of composition C_1, C_2 and C_3, respectively. In alloys containing 3.28% V and 4.73% V, chromium and iron atoms have been substituted by vanadium in all three different compositions of eutectic carbides. In cases of C_1 and C_2 carbies greater number of chromium atoms were substituded by vanadium, while in carbides C_3 greater number of iron atoms have been substituted [27].

In the earlier studies [21,54–57] it has been noticed that Fe/Cr ratio in eutectic carbides depends on carbon content in alloys with the same chromium content (hypoeutectic, eutectic and hypereutectic type alloy) or on the cooling rate. Doğan *et al*. [54] did observe that while the Fe/Cr ratio of atomic fraction in the M_7C_3 carbide of hypoeutectic and eutectic high chromium white iron with 15% Cr is approximately 1, it is 1.3 in 15% Cr hypereutectic iron. Jacuinde [57] has found in the study of iron containing 16.9% Cr, 2.58% C and 1.98% V that for higher cooling rate Fe/Cr ratio is 1.36, and that for slower cooling rate Fe/Cr ratio is 0.97.

Different morphologies of eutectic colonies in the columnar zone of as-cast structure of Fe–Cr–C–V white irons presented in Figs. 4 and 5. The eutectic colony consists of carbides of different compositions (Table 4 and Fig. 4). Blade-like carbides predominantly show C_3 composition [27].

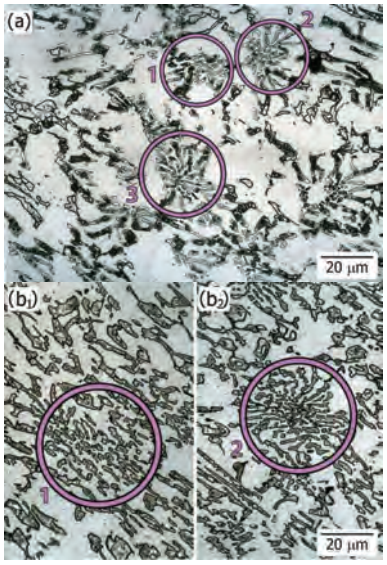

Fig. 5. Optical micrographs of hypoeutectic Fe–Cr–C iron (a) and Fe–Cr–C–V iron containing 3.28% V (b_1 and b_2) in the columnar zone of as-cast structures (5 mm from the surface). Different morphologies of eutectic colonies are marked by 1 to 3.

In the columnar zone of as-cast structures, the eutectic carbides are usually aligned so that the long axis of the carbide rods is parallel with the direction of heat flow (*i.e*., perpendicular to the cast surface), forming a highly anisotropic morphology. The formation of eutectic colonies of different morphologies is assumed to be related to the segregation of alloying elements in the melt. That is confirmed by EDS analysis which indicates different M_7C_3 carbide compositions (Table 4).

Table 4. Chemical composition of M_7C_3 eutectic carbide in Fe–Cr–C–V alloys (mass%). The values are based on an average of thirty different measurements per each of three different chemical compositions of M_7C_3 eutectic carbide in all tested alloys

Alloy	M_7C_3	Element								Formula
		C	Si	Mn	Mo	Cu	Cr	Fe	V	
1	C_1	8.17	0.028	0.673	0.557	0.032	53.36	38.07	–	$Cr_{4.2}Fe_{2.8}C_3$
	C_2	8.55	0.033	0.548	0.674	0.047	45.44	44.68	–	$Cr_{3.6}Fe_{3.3}C_3$
	C_3	8.43	0.019	0.659	0.494	0.053	39.77	50.11	–	$Cr_{3.2}Fe_{3.8}C_3$
2	C_1	8.35	0.031	0.781	0.595	0.020	53.12	37.91	0.111	$Cr_{4.2}Fe_{2.8}C_3$
	C_2	8.18	0.014	0.487	0.538	0.045	45.88	45.29	0.076	$Cr_{3.6}Fe_{3.3}C_3$
	C_3	8.67	0.028	0.663	0.686	0.038	38.87	51.18	0.078	$Cr_{3.1}Fe_{3.8}C_3$
4	C_1	8.23	0.011	0.667	0.541	0.049	48.43	38.13	3.63	$Cr_{3.8}Fe_{2.8}V_{0.3}C_3$
	C_2	8.48	0.032	0.535	0.672	0.029	42.72	44.22	2.76	$Cr_{3.4}Fe_{3.3}V_{0.2}C_3$
	C_3	8.41	0.055	0.671	0.479	0.048	38.72	48.93	2.75	$Cr_{3.1}Fe_{3.6}V_{0.2}C_3$
6	C_1	8.56	0.045	0.461	0.451	0.059	45.46	34.54	10.62	$Cr_{3.6}Fe_{2.6}V_{0.8}C_3$
	C_2	8.62	0.027	0.675	0.564	0.037	38.53	43.92	7.74	$Cr_{3.1}Fe_{3.2}V_{0.6}C_3$
	C_3	8.28	0.029	0.427	0.448	0.056	35.52	46.01	8.35	$Cr_{2.8}Fe_{3.4}V_{0.7}C_3$
7	C_1	8.44	0.016	0.585	0.671	0.061	43.16	32.97	14.19	$Cr_{3.4}Fe_{2.4}V_{1.1}C_3$
	C_2	8.14	0.031	0.643	0.451	0.048	38.03	40.92	11.79	$Cr_{3.0}Fe_{3.0}V_{0.9}C_3$
	C_3	8.37	0.013	0.591	0.493	0.053	34.19	45.24	11.53	$Cr_{2.7}Fe_{3.4}V_{0.8}C_3$

During solidification, solute segregation will influence nucleation and growth kinetics through its influence on constitutional undercooling (the constitutional undercooling of a particular phase is dependent on the *liquidus* and/or eutectic temperature which, in turn, is dependent on the local liquid composition) [27]. Due to different melt composition in particular regions, the constitutional undercooling and also the growth rate are different and the formation of eutectic colonies with different morphologies will be induced (Figs. 4 and 5).

According to solidification theory [51], for a hypoeutectic alloy composition, the alloy *liquidus* is much higher than the eutectic temperature. Thus the corresponding primary phase is highly constitutionally undercooled, due to the long-range boundary layer built up ahead of the solid–liquid interface in this case, and tends to grow faster than the eutectic. Consequently, primary phase will destabilize the solid–liquid interface. At the time when eutectic nucleation and growth occur, the conditions in the melt will in part be imposed by the characteristics of the previous reaction [52]. Since it can be assumed that thermal conditions, such as thermal gradient and cooling rate, are the same, the morphology of the eutectic growth front will depend on melt composition in particular zones. In the regions with a smaller content of alloying elements, the rosette-like eutectic colonies in which carbides are located radially from the center will be formed (Fig. 4d), whereas in regions of enriched melt, the formation of eutectic colonies consisting of a larger number of long M_7C_3 carbide rods will be favored (Fig. 4a).

The morphology of the eutectic carbides vary from the center to the edge of eutectic colonies marked by 1 and 2 in Figs. 4 and 5. The rod shaped carbides are finer at the center of the eutectic colony and become coarser rod-like or blade-like with increased distance from the center (Fig. 4b and c), as indicates that eutectic solidification begins at the center with a certain undercooling and proceeds radially outward. As solidification progresses, the constitutional undercooling decreases, and thus the rod-like or blade-like carbides that form during the later stages of solidification are coarser [27].

This can be explained by the fact that, during M_7C_3/γ eutectic growth, the solute atoms (as carbon, chromium and vanadium), which are rejected by one phase, are usually needed for the growth of the other. Therefore, lateral diffusion along the solid-liquid interface perpendicular to the growth direction, will become dominant and effectively decreases the solute build-up (ΔC) ahead of both phases. This lateral diffusion causes the interphase spacing, λ, in the eutectic structure to be decreased. However, as λ decreases, an opposing force (capillary effect), which arises from the increased energy associated with the increased curvature of the solid/liquid interface, comes into effect. As shown in Fig. 6, the diffusion effect can be expressed in terms of a constitutional undercooling (ΔT_c) while the latter can be expressed in terms of a curvature undercooling (ΔT_r) [27,51,52]. The sum of the solute (ΔT_c) and curvature (ΔT_r) undercoolings must therefore equal the interface undercooling, ΔT. Both undercoolings vary with λ in opposite ways: ΔT_c, which is proportional to ΔC (the driving force for solute diffusion) increases with λ, while ΔT_r decreases. The interphase spacing in the eutectic structure is eventually established by the equilibrium between an attractive force arising from the diffusion effect and a repulsive force arising from the curvature effect. Decrease in growth rates will shift ΔT_c to ΔT_{c1} without changing the ΔT_r curve, leading to a higher spacing value, λ_1. It is also evident from Fig. 6 that for small values of λ, eutectic growth is controlled by capillary effects ($\Delta T_r > \Delta T_c$), while diffusion is the limiting process at large spacing values [51,58]. With increasing λ values the size of M_7C_3 carbides increases.

In the case of eutectic colonies marked 3 in Figs. 4d and 5a, eutectic grows uniformly in all directions and finally a rosette-like structure is obtained.

The morphology of particular M_7C_3 carbides in Fe––Cr–C–V alloys does not significantly change with increasing vanadium content. These carbides are rod or blade shaped. The volume fraction, size and distribution of rod-like and blade-like carbides in the eutectic colonies are changing with increasing vanadium content in the alloy (Fig. 5). The rod type morphology of eutectic carbides is more dominant in Fe–Cr–C–V alloys with higher content of vanadium. These changes in morphology can be explained by the fact that in alloy with higher vanadium content, due to the higher concentration of vanadium in the melt, and subsequently larger constitutional undercooling, the growth rate is faster than in alloys with lower vanadium content, under the same cooling conditions [27].

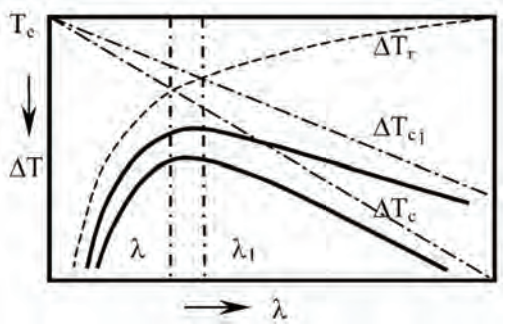

Fig. 6. Adjustment of interphase spacing during eutectic growth.

As-cast matrix microstructure

Vanadium was found to affect the transformation of austenite in as-cast condition of a Fe–Cr–C–V white irons [33]. Changes in the matrix microstructure over

the examined range of vanadium levels are illustrated in Fig. 1.

The austenite remains as a metastable phase at room temperature in Fe–Cr–C alloy with no vanadium addition [1] and Fe–Cr–C–V alloy containing 0.12% V (Figs. 1a), due to the high amount of carbon and alloying elements that lowers the martensite transformation starting temperature M_s.

The inhomogeneity of the dendrites in Fe–Cr–C–V alloys containing 0.49–4.73% V can be clearly seen (Fig. 1b–d). Fine dark particles predominantly located in the middle zone of the austenite (Fig. 1b–d) were identified to be carbides of $M_{23}C_6$ type (Fig. 7a). TEM observation revealed that the secondary carbides were distributed in a regular series (Fig. 7a and b), indicating a precipitation along preferred crystallographic planes. Around the carbide particles, the presence of dislocations (Fig. 7b) or martensite (Fig. 7b and c) was noticed.

As it can be seen from Fig. 1a–c, in alloys containing less than 3.28% V, primary and eutectic austenite is transformed in a narrow zone along the border with eutectic M_7C_3 carbide.

It has been suggested by several authors [1,13,21, 33,39] that during eutectic solidification the M_7C_3 carbide, which grows along the austenite, absorbs carbon from its surroundings and a narrow area at the austenite/carbide interphase becomes impoverished in it. The lack of carbon in these zones of austenite increases the M_s temperature which allows these areas of austenite to transform into martensite, during subsequent cooling.

Nevertheless, in Fe–Cr–C–V alloys containing 3.28 (Fig. 1d) and 4.73% V [33], a remarkably higher degree of austenite transformation can be seen. TEM Analysis identified martensite as a product of this transformation [33].

The chemical composition of austenite changes by changing the vanadium content in high chromium iron (Table 5). Adding more vanadium into the Fe–Cr–C–V type alloys was followed by higher vanadium content in the austenite, as a normal consequence of its wide solubility range in the *γ*-solid solution. The lower carbon content experienced in the matrix in alloy with higher vanadium content was assumed to be related to the larger amount of eutectic with M_7C_3 carbides (Table 3).

At temperatures below solidus, in the course of further cooling after solidification, $M_{23}C_6$ carbides precipitate in austenite (Fig. 7), mainly in areas with lower carbon content. Due to heterogeneity of the matrix composition, the precipitation is heterogeneous, and in alloys with vanadium content lower than 2% they were predominantly located in the surface dendrite zone (Fig. 1b and c).

The carbides precipitation kinetic in austenite of Fe–Cr–C–V alloys depends on the vanadium content in the alloy [33]. In spite of the vanadium content increase in the austenite matrix, the part of the added vanadium was locked in the precipitated $M_{23}C_6$ carbides, whose volume fraction increased in alloys with higher vanadium content.

The transformation of austenite into martensite in the Fe–C–Cr–V alloys is closely related to the precipitation of secondary carbides. Precipitation of $M_{23}C_6$ carbides minimizes the carbon and chromium content in the matrix, and increases the M_s temperaature. The degree of martensitic transformation is determined by the amount of precipitated carbides, i.e. depends on the austenite composition [33].

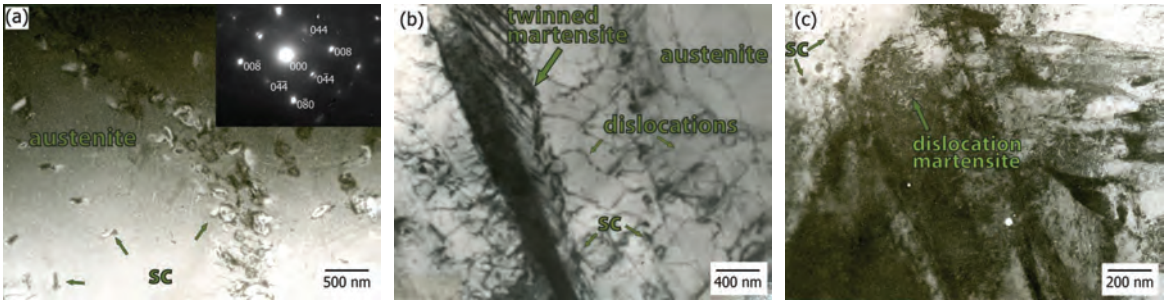

Fig. 7. TEM Micrographs of the Fe–C–Cr–V alloy containing 1.19% V showing: a) secondary carbides and selected-area diffraction pattern (in the corner) from the region in this micrograph showing a [100] zone axis; b) and c) secondary carbides and martensite.

Table 5. Chemical composition of the as-cast matrix in Fe–C–Cr–V alloys (mass%)

Alloy	V in alloy, mass%	Element							
		C	Si	Mn	Mo	Cu	Cr	Fe	V
2	0.12	1.35–1.56	0.82–0.93	0.63–0.68	0.24–0.34	1.43–1.81	11.76–12.89	82.07–83.16	0.014–0.015
4	1.19	1.01–1.31	0.95–1.12.	0.78–0.82	0.22–0.38	1.46–1.82	11.20–12.71	82.92–83.24	0.341–0.346
6	3.28	0.65–0.94	0.88–0.97	0.72–0.81	0.17–0.35	1.74–1.96	11.51–12.42	81.37–82.84	1.26–1.29
7	4.73	0.54–0.79	0.96–1.04	0.78–0.81	0.32–0.47	1.71–1.87	11.62–12.16	81.14–82.35	1.84–1.89

The amount of retained austenite in the Fe–Cr–C–V white irons is found to decrease with increasing vanadium content (Fig. 8).

Microstructure after subcritical heat treatment

After heat treatment (500 °C/4 h) there were no notable changes in the structure of a basic Fe–Cr–C white iron [2, 13]. However, during isothermal holding at 500 °C for 4 h, the secondary carbides precipitated in the austenite of Fe–Cr–C–V white irons. Martensite present in the as-cast structure was also tempered at this temperature. Austenite was then partly transformed into martensite during the cooling process. The amount of precipitated carbides and volume fraction of martensite which formed depended on the basic as-cast structure, *i.e.*, on vanadium content in the alloy [2].

EFFECT OF MICROSTRUCTURE ON THE PROPERTIES OF TESTED Fe-Cr-C-V ALLOYS

Vanadium therefore altered the microstructure characteristics of high chromium white cast iron and affected its properties.

Effect of microstructure on the hardness of tested Fe–C–Cr–V alloys

The matrix microhardness and the alloy macrohardness were improved by increasing the vanadium content in both the as-cast and heat treated state (Figs. 9 and 10).

The improved hardness of the Fe–C–Cr–V white irons by increasing vanadium content in as-cast condition (Fig. 10) was the result of an increased volume

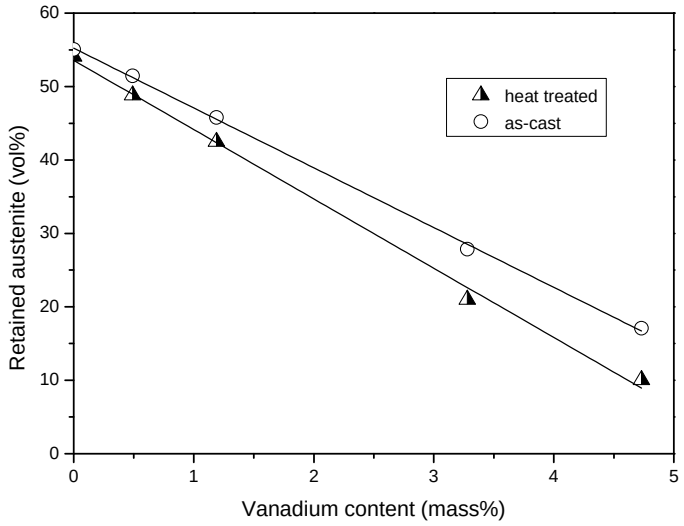

Fig. 8. Volume fraction of retained austenite as a function of vanadium content in Fe–Cr–C–V white irons in both as-cast and heat treatment state.

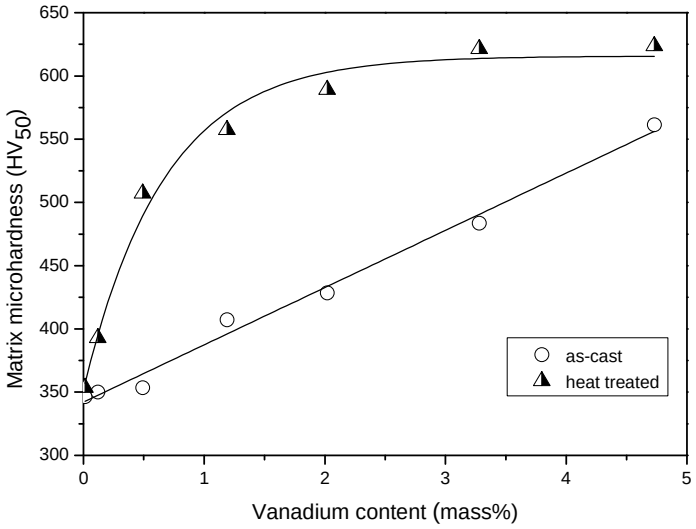

Fig. 9. Matrix microhardness as a function of vanadium content in Fe–Cr–C–V white irons in both as-cast and heat treatment state.

fraction of the eutectic M_7C_3 and V_6C_5 carbide. Nevertheless, an increase in the amount of precipitated carbides in austenite and the formation of a larger amount of martensite, combined with a reduction in the volume fraction of retained austenite (Fig. 8), improved the matrix microhardness (Fig. 9), and consequently the alloy macrohardness (Fig. 10) in both the as-cast and heat treated states [29].

Effects of microstructure on the abrasion wear resistance of tested Fe–C–Cr–V alloys

The influence of vanadium on abrasion resistance* is presented in Fig. 11. Wear resistance improved as the concentration of vanadium increased up to 3.28%, and fell off thereafter. Abrasion wear resistance was slightly higher after heat treatment at 500 °C (Fig. 11).

The abrasion resistance of the carbide phase was more effective than the matrix in white cast irons, since, mainly, the hardness of M_7C_3 (1200–1800 HV [1]) carbides were greater than the hardness of the used abrasive – quartz (900-1080 HV [1]). In white cast irons the matrix was preferentially worn by a cutting action, under low-stress abrasion conditions. Eutectic carbides were then forced to stand in relief and directly obstruct the cutting action of abrasive particles for a period of time until they were partly or completely removed by a

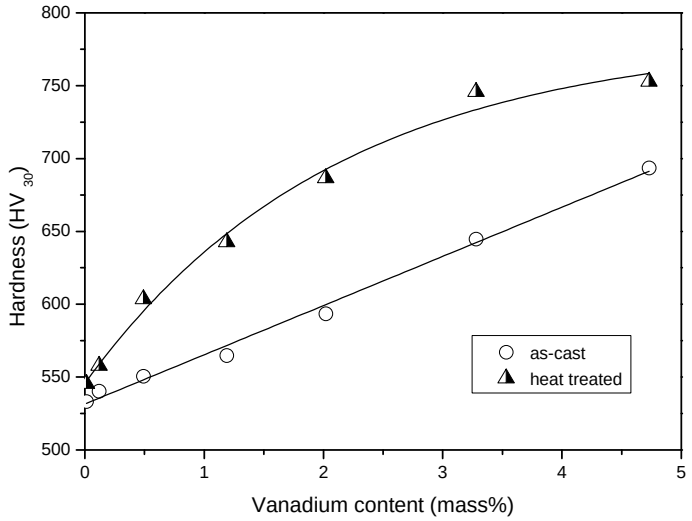

Fig. 10. Hardness as a function of vanadium content in Fe–Cr–C–V white irons in both as-cast and heat treatment state.

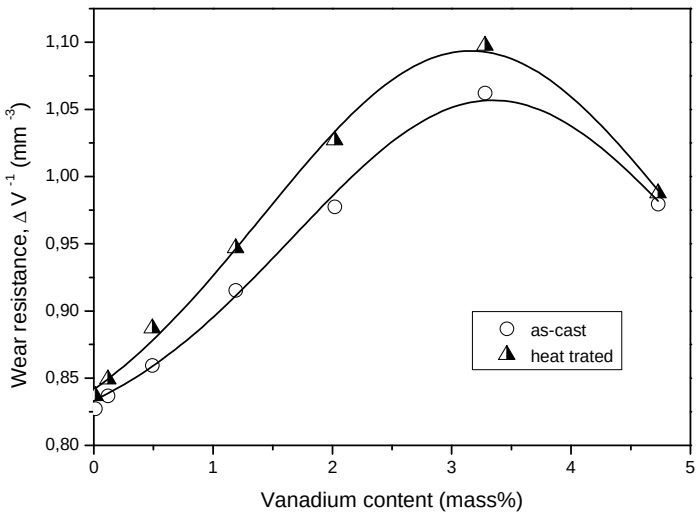

Fig. 11. Wear resistance as a function of vanadium content in Fe–Cr–C–V white irons in both as-cast and heat treatment state.

*Abrasive wear resistance was evaluated according to the ASTM Standard Practice G-65, Procedure B (Dry Sand/Rubber Wheel Abrasion Test).

cutting or chipping action [1,5,29]. In other words, wear under low-stress abrasion conditions, and using a quartz abrasive, was apparently controlled by the rate of removal of the carbide phase since the protruding

carbides protected the matrix from direct attack of abrasive particles [2].

Therefore, increasing the volume fraction of M_7C_3 eutectic carbides up to 35% in the Fe–C–Cr–V white irons, and simultaneously increasing the amount of very hard V_6C_5 carbide (2800 HV), reduced the volume loss caused by abrasive wear (Fig. 11). However, a further increase in the volume fraction of the carbide phase (alloy with 4.73% V, Table 3) reduced wear resistance (Fig. 11), which was most likely attributable to intensive spalling of massive carbides during wear.

In addition to the volume fraction of carbides, the size of phases present in the structure was another microstructure variable which affected the abrasive resistance of the Fe–Cr–C–V alloys. The smaller size of primary austenite dendrites, *i.e.*, the average distance between carbide particles, caused by increasing the content of vanadium in the alloy (Table 3), protected the matrix better from direct attack by abrasive particles. The shorter rods of M_7C_3 carbides (Table 3) also tended to be less severely cracked during wear, thereby improving the wear resistance of the alloys. It must be specified, however, that the effect of controlling wear rate by refining the microstructure depended on abrasive grit size, *i.e.*, the ratio of mean free path to mean abrasive asperity size [4,13,29]. The smaller the ratio, the less likely that grit would undermine the hard particles by penetrating the matrix.

The improved wear resistance of white cast irons after heat treatment, compared with the as-cast condition (Fig. 11) indicated that wear resistance under low-stress abrasion conditions also depended on the matrix microstructure. In addition to the fact that the matrix helped control of the penetration depth of abrasive particles, it also played an important role in preventing bodily removal of smaller carbides and cracking of massive ones [14]. Experimental results indicate that the martensitic or martensite-austenitic matrix microstructure more adequately reinforced M_7C_3 eutectic carbides to minimize cracking and removal during wear than the austenitic matrix [29].

Besides, the secondary carbides which precipitate in the matrix regions of high chromium white irons also influence the abrasion behaviour [2,25]. By increasing the matrix strength through a dispersion hardening effect, the fine secondary carbides can increase the mechanical support of the eutectic carbides. These results agree with those of Liu et al. [59] and Wang et al. [60] who found that the precipitation of fine $M_{23}C_6$ carbides and the more homogeneous carbide distribution as a result of cryogenic treatment is responsible for the improved wear resistance of high chromium white irons.

Effect of microstructure on the fracture toughness of tested Fe–C–Cr–V alloys

The higher content of vanadium in high chromium white iron increases the volume fraction of the carbide phase and reduces fracture toughness. On the other hand, the toughness has been improved by reducing the size of M_7C_3 eutectic carbide. However, the results of fracture toughness tests* in both as-cast and heat treated conditions (Fig. 12) show that the dynamic fracture toughness in white cast irons is determined

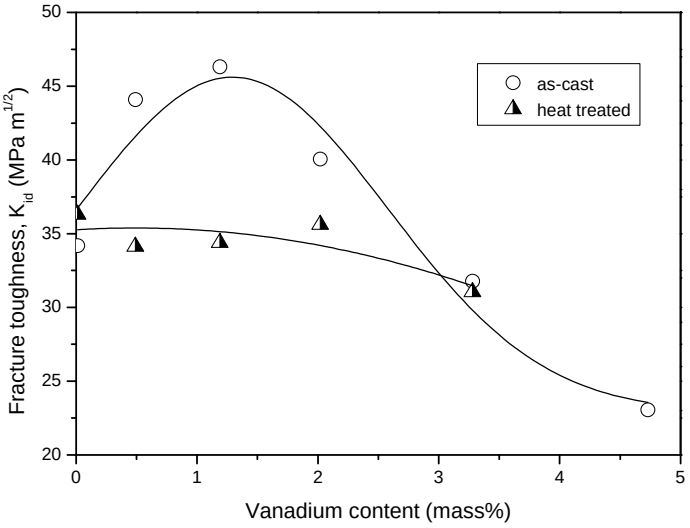

Fig. 12. Fracture toughness as a function of vanadium content in Fe–Cr–C–V white irons in both as-cast and heat treatment state.

*Dynamic fracture toughness was measured at room temperature using an impact test machine equipped with an instrumented Charpy tub. The testing methodology selected was based on the three-point bending tests. The specimens of 10 mm×10 mm×55 mm in size, were notched and precracked by fatigue following ASTM E399 standard.

mainly by the properties of the matrix. The austenite is more effective in this respect than martensite [2,29].

By increasing the vanadium content, the amount of retained austenite decreased, as it shown in Fig. 8, which subsequently reduced toughness. However, the Fe–C–Cr–V alloys containing 1.19% V in the as-cast condition, showed greater dynamic fracture toughness when compared to the basic Fe–C–Cr alloy, Fig. 12. Fracture toughness was determined mainly by the energy that had to be consumed in extending the crack through ligaments of matrix [10,36]. Since the austenite in that alloy contained very fine $M_{23}C_6$ carbide particles, higher fracture toughness was attributed to a strengthening of the austenite during fracture [29]. Hence, the contribution to improving the fracture toughness of the alloy containing 1.19 wt.% V, due to the presence of fine $M_{23}C_6$ carbides within the austenite, was considerably higher than the reduction. Reduction was caused by, on the one hand, increasing the amount of M_7C_3 carbides and reducing inter-carbide distance, and on the other hand, reducing the volume fraction of retained austenite. Where the content of vanadium exceeded 1.19%, fracture toughness decreased (Fig. 12), since the matrix microstructure of those alloys was mainly martensitic.

In heat-treated Fe–C–Cr–V alloys with varying contents of vanadium, lower K_{id} values wear obtained, compared with as-cast alloys (Fig. 12). Several processes which occurred during tempering affected fracture toughness. When held at 500 °C for 4 h, extensive carbide precipitation probably occurred in the martensite present in the as-cast structure, and retained austenite was decomposed [2,13]. Both effects combined to produce a significant drop in fracture toughness. Furthermore, during the cooling process, after it had been held at the tempering temperature, martensite formed, which also contributed to lower K_{id} values.

Effect of microstructure on the impact resistance of tested Fe–C–Cr–V alloys

The results obtained by examination of impact resistance* of Fe–Cr–C–V white irons in as-cast condition are presented in Fig. 13.

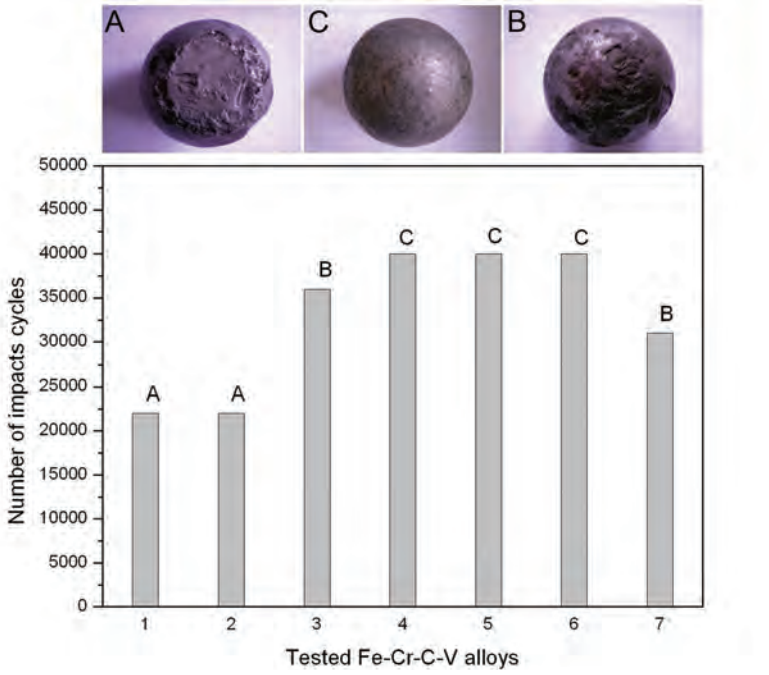

Fig. 13. Impact resistance of Fe–Cr–C–V white irons in as-cast condition. Markings on the graph: A – form of the balls changed, balls gained an elliptic shaped; B – spalling of the balls started; C – testing interrupted, form unchanged and no spalling of the balls.

Fe–Cr–C–V white irons show considerably higher impact resistance compared to the basic Fe–Cr–C white iron (Fig. 13). However, the vanadium content influence on the impact resistance was not unique, as the importance of the specific structural features brought by adding vanadium indicates [26].

*The impact resistance of Fe–Cr–C–V white irons was tested using an impact-fatigue test machine. The test balls (ten balls of each examined alloy) were lifted to a height of up to 6.4 m and allowed to fall freely on the hardened steel anvil. Following impact, each ball was automatically recycled, by means of a bucket-type elevator, and allowed to drop again on the anvil. The impact cycles were repeated until the ball failed (defined either by the ball cracking or the appearance of significant spalls). The number of impacts to failure was taken as a measure of the impact resistance.

TEM Micrographs of the surface layer (4 mm depth from ball surface) of a Fe–Cr–C–V alloy ball, containing 1.19% V, after impact resistance testing, are shown in Fig. 14. In the surface dendritic area, along the border with M_7C_3 carbides, austenite was transformed into martensite (Fig. 14a), and this change was rather similar before and after the impact resistance testing (Fig. 1c).

Micrographs in Fig. 14b and c indicate a clear planar deformation substructure. In the austenitic matrix very fine twinning lamellae (width about 50–60 nm) can be observed, due to the twinning occurring on {111} planes (making the angle ≈70°), and a planar dispositional arrangement produced by slip at the same slip system (Fig. 14b and c).

The hardness was measured at 4 mm depth from ball surface of the Fe–Cr–C–V cast iron containing 1.19% V was 668 HV before the impact test, increasing to the range from 936 to 984 HV, after the test.

The fact that in Fe–Cr–C–V alloys with increasing vanadium content the retained austenite volume fraction decreases (Figs. 1 and 8), the amounts of precipitated $M_{23}C_6$ carbides and martensite increase (Fig. 1), and the fact that the impact resistance of the alloys with 0.49% V and 1.19–3.28% V is 60 and 80% higher, respectively, compared to basic Fe–Cr–C alloy (Fig. 13), indicates the complexity of the hardening process in tested balls.

Deformed substructure revealed in the retained austenite at the surface of the ball after impact test (Fig. 14), indicates that under repeated impact loading, deformation and appropriate strain hardening come into play [26]. The emergence of fine twinning lamellae as a primary deformation mechanism and subsequent activation of planar slip of dislocations are considered to be anomalies in deformation behaviour of austenitic steels with low-stacking-fault energy, which may result in a very strong strain hardening effect [61]. According to the results of TEM examinations (Fig. 14b and c), it was supposed that similar activity of an anomalous strain hardening happened in the retained austenite of the tested balls of high chromium white cast iron alloyed with vanadium. The change in the amount of austenite was assumed to affect the strain hardening process, and obviously in the white iron with 4.73% V the strain hardening effect was weak due to a little retained austenite (Fig. 8).

The particles of precipitated $M_{23}C_6$ secondary carbides disturb dislocations movement and contribute to increase the effects of strain hardening in Fe–Cr–C–V white irons [26].

According to literature [3], the impact resistance of Fe–Cr–C white iron with high chromium content decreases with increasing volume fraction of eutectic M_7C_3 carbides. Nevertheless, in Fe–Cr–C–V white cast irons, regardless of the increased amount of eutectic carbides in the structure, the higher impact resistance for higher vanadium content in alloy up to 3.28% V, can be related to the strain hardening of retained austenite [26]. The alloy with 4.73% V shows a lower impact resistance compared to other Fe–Cr–C–V alloys and it was assumed to be the consequence of, on one hand, the lower amount of retained austenite and the higher amount of martensite and, on the other hand, of a large volume fraction of eutectic M_7C_3 carbides. Thus, the lower impact resistance found in balls with 4.73% V obviously is the result of a complex interaction of all structural features and hardening phenomena.

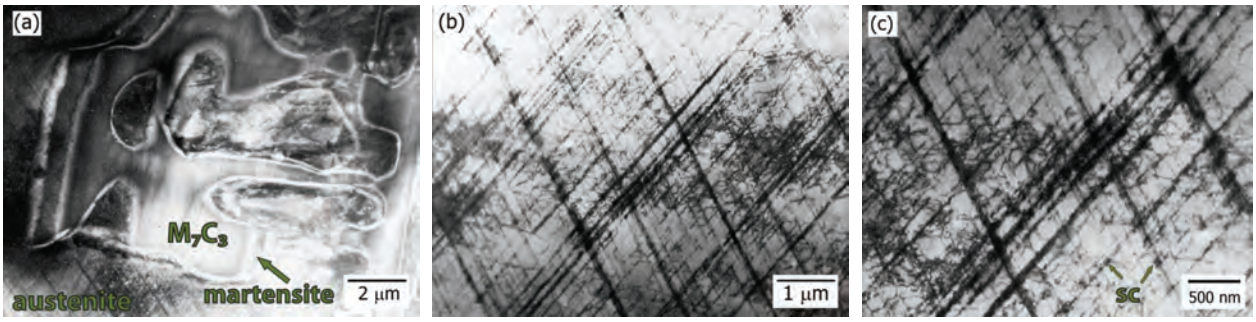

Fig. 14. TEM Micrographs of Fe–C–Cr–V white iron containing 1.19% V after impact resistance testing.

CONCLUSIONS

The microstructure of Fe–Cr–C–V white irons consists of M_7C_3 and vanadium rich M_6C_5 carbides in austenitic matrix.

With an increase of vanadium content the alloy composition approaches the eutectic composition in the quaternary Fe–Cr–C–V system, causing a decrease of the solidification temperature interval, and thereby also changing the volume fraction, size and morphology of the present phases. Vanadium changes the transformation characteristics of austenite in as-cast condition in the Fe–C–Cr–V type alloys. The transformation of austenite to martensite in the Fe–C–Cr–V is closely connected with the secondary carbide deposition.

The volume fraction of the carbide phase, carbide size and distribution had an important influence on the wear resistance of Fe–Cr–C–V white cast iron alloys under low-stress abrasion conditions. However, the dynamic fracture toughness of Fe–Cr–C–V white cast irons is determined mainly by the properties of the matrix. The austenite is more effective in this respect than martensite. Since the austenite in these alloys contained very fine $M_{23}C_6$ carbide particles, higher fracture toughness was attributed to a strengthening of the austenite during fracture. Besides, the secondary carbides which precipitate in the matrix regions also influence the abrasion behaviour. By increasing the matrix strength through a dispersion hardening effect, the fine secondary carbides can increase the mechanical support of the carbides. Deformation and appropriate strain hardening occur in the retained austenite of Fe–Cr–C–V alloys under repeated impact loading. The particles of precipitated $M_{23}C_6$ secondary carbides disturb dislocations movement and contribute to increase the effects of strain hardening in Fe–Cr–C–V white irons.

It was therefore possible, by adding approximately 3 wt.% V to high chromium white iron, to obtain an alloy that will have, in the as-cast condition or after tempering at 500 °C, better properties than high temperature treated alloys with no vanadium addition. This may be very important from a practical point of view, especially for castings with a complex configuration, since the possibility of high residual stresses during high temperature heat treatment and problems related to this process can be avoided.

REFERENCES

[1] C.P. Tabrett, I.R. Sare, M.R. Ghomashchi, Microstructure–property relationships in high chromium white iron alloys, Int. Mater. Rev. **41** (1996) 59–82.

[2] M. Filipovic, Z. Kamberovic, M. Korac, M. Gavrilovski, Correlation of microstructure with the wear resistance and fracture toughness of the white cast iron alloys, Met. Mater. Int. **19** (2013) 473–481.

[3] I.R. Sare, B.K. Arnold, G.A. Dunlop, P.G. Lloyd, Repeated impact-abrasion testing of alloy white cast irons, Wear **162–164** (1993) 790–801.

[4] I.R. Sare, Abrasion resistance and fracture toughness of white cast irons, Met. Technol. **6** (1979) 412–419.

[5] K.H. Zum Gahr, D.V. Doane, Optimizing fracture toughness and abrasion resistance in white cast irons, Metall. Trans., A **11** (1980) 613–620.

[6] C.K. Kim, S. Lee, J.Y. Jung, Effects of heat treatment on wear resistance and fracture toughness of duo-cast materials composed of high-chromium white cast iron and low-chromium steel, Met. Mat. Trans., A **37** (2006) 633–643.

[7] A. Wiengmoon, J.T.H. Pearce, T. Chairuangsri, Relationship between microstructure, hardness and corrosion resistance in 20 wt.% Cr, 27 wt.% Cr and 36 wt.% Cr high chromium cast irons, Mater. Chem. Phys. **125** (2011) 739–748.

[8] Ö.N. Doğan, Columnar to equiaxed transition in high Cr white iron castings, Scr. Mater. **35** (1996) 163–168.

[9] Ö.N. Doğan, J.A. Hawk, Effect of carbide orientation on abrasion of high Cr white cast iron, Wear **189** (1995) 136–142.

[10] G. Powell, V. Randle, The effect of Si on the relationship between orientation and carbide morphology in high chromium white irons, J. Mater. Sci. **32** (1997) 561–565.

[11] R. Correa, A. Bedolla-Jacuinde, J. Zuno-Silva, E. Cardoso, I. Mejía, Effect of boron on the sliding wear of directionally solidified high-chromium white irons, Wear **267** (2009) 495–504.

[12] J.J. Coronado, Effect of load and carbide orientation on abrasive wear resistance of white cast iron, Wear **270** (2011) 287–293.

[13] I.R. Sare, B.K. Arnold, The influence of heat treatment on the high-stress abrasion resistance and fracture toughness of alloy white cast irons, Met. Mater. Trans. **26** (1995) 1785–1793.

[14] C.P. Tabrett, I.R. Sare, Fracture toughness of high-chromium white irons: Influence of cast structure, J. Mater. Sci. **35** (2000) 2069–2077.

[15] A. Kootsookos, J.D. Gates, The role of secondary carbide precipitation on the fracture toughness of a reduced carbon white iron, Mater. Sci. Eng., A **490** (2008) 313––318.

[16] A. Sawamoto, K. Ōgi, K. Matsuda, Solidification structures of Fe–C–Cr–(V–Nb–W) alloys, AFS Trans. **94** (1986) 403–416.

[17] S.H. Mousavi Anijdan, A. Bahrami, N. Varahram, P. Davami, Effects of tungsten on erosion–corrosion behavior of high chromium white cast iron, Mater. Sci. Eng., A **454–455** (2007) 623–628.

[18] H.K. Baik, C.R. Loper, The influence of niobium on the solidification structure of Fe-C-Cr alloys, AFS Trans. **96** (1988) 405-412.

[19] C.R. Loper, H.K. Baik, Influence of molybdenum and titanium on the microstructures of Fe-C-Cr-Nb white cast irons, AFS Trans. **97** (1989) 1001–1008.

[20] M. Fiset, K. Peev, M. Radulovic, The influence of niobium on fracture toughness and abrasion resistance in high chromium white cast irons, J. Mater. Sci. Lett. **12** (1993) 615–617.

[21] A. Bedolla-Jacuinde, Microstructure of vanadium-, niobium- and titanium-alloyed high-chromium white cast irons, Int. J. Cast Metals Res. **13** (2001) 343–361**.**

[22] R. Kesri, M. Durand-Charre, Phase equilibria, solidification and solid-state transformations of white cast irons containing niobium, J. Mater. Sci. **22** (1987) 2959––2964.

[23] X. Zhi, J. Xing, H. Fu, B. Xiao, Effect of niobium on the as-cast microstructure of hypereutectic high chromium cast iron, Mater. Lett. **62** (2008) 857–860.

[24] G.H. Coelho, J.A. Golczewski, H.F. Fischmeister. Thermodynamic calculations for Nb-containing high-speed steels and white cast iron alloys, Met. Mat. Trans., A **34** (2003) 1749–1758.

[25] M. Filipovic, Z. Kamberovic, M. Korac, M. Gavrilovski, Microstructure and mechanical properties of Fe–Cr–C––Nb white cast irons, Mater. Des. **47** (2013) 41–48.

[26] M. Filipovic, E. Romhanji, Strain hardening of austenite in Fe–Cr–C–V alloys under repeated impact, Wear **270** (2011) 800–805.

[27] M. Filipovic, E. Romhanji, Z. Kamberovic, Chemical composition and morphology of M_7C_3 eutectic carbide in high chromium white cast iron alloyed with vanadium, ISIJ Int. **52** (2012) 2200–2204.

[28] J.D.B. De Mello, M. Durand-Charre, T. Mathia, Abrasion mechanisms of white cast iron II: Influence of the metallurgical structure of V–Cr white cast irons, Mater. Sci. Eng. **78** (1986) 127–134.

[29] M. Radulovic, M. Fiset, K. Peev, M. Tomovic, The influence of vanadium on fracture toughness and abrasion resistance in high chromium white cast irons, J. Mater. Sci. **29** (1994) 5085–5094.

[30] A. Bedolla-Jacuinde, L. Arias, B. Hernández, Kinetic of secondary carbides precipitation in a high-chromium white iron, J. Mater. Eng. Perform. **12** (2003) 371–382.

[31] A. Wiengmoon, T. Chairuangsri, J.T.H. Pearce, Microstructural and crytallographical study of carbides in 30wt.%Cr cast irons, Acta Materialia **53** (2005) 4143––4154.

[32] J. Wang, R.L. Zuo, Z.P. Sun, C. Li, K.K. Liu, H.X. Yang, B.L. Shen, S.J. Huang, Influence of secondary carbides precipitation and transformation on hardening behavior of a 15 Cr–1 Mo–1.5 V white iron, Mater. Charact. **55** (2005) 234–240.

[33] M. Filipovic, E. Romhanji, Z. Kamberovic, M. Korac, Matrix microstructure and its micro-analysis of constituent phases in as-cast Fe–Cr–C–V alloys, Mater. Trans. **50** (2009) 2488–2492.

[34] M. Filipovic, Z. Kamberovic, M. Korac, Solidification of high chromium white cast iron alloyed with vanadium, Mater. Trans. **52** (2011), 386–390.

[35] X. Wu, J. Xing, H. Fu, X. Zhi, Effect of titanium on the morphology of primary M_7C_3 carbides in hypereutectic high chromium white iron, Mater. Sci. Eng., A **457** (2007) 180–185.

[36] X. Zhi, J. Xing, H. Fu, Y. Gao, Y, Effect of titanium on the as-cast microstructure of hypereutectic high chromium cast iron, Mater. Charact. **59** (2008) 1221–1226.

[37] A. Bedolla-Jacuinde, R. Correa, I. Mejia, J.G. Quezada, W.M. Rainforth, The effect of titanium on the wear behaviour of a 16% Cr white cast iron under pure sliding, Wear **263** (2007) 808–820.

[38] X. Wu, J. Xing, H. Fu, X. Zhi, Effect of titanium on the morphology of primary M_7C_3 carbides in hypereutectic high chromium white iron, Mater. Sci. Eng., A **457** (2007) 180–185.

[39] A. Bedolla-Jacuinde, R. Correa, J.G. Quezada, C. Maldonado, Effect of titanium on the as-cast microstructure of a 16% chromium white iron, Mater. Sci. Eng., A 398 (2005) 297–308.

[40] Y. Taşgin, M. Kaplan, M. Yaz, Investigation of effects of boron additives and heat treatment on carbides and phase transition of highly alloyed duplex cast iron, Mater. Des. **30** (2009) 3174–3179.

[41] J.W. Choi, S.K. Chang, Effects of molybdenum and copper additions on microstructure of high chromium cast iron rolls, ISIJ Int. **32** (1992) 1170–1176.

[42] C. Scandian, C. Boher, J.D.B. De Mello, F. Rézaï-Aria, Effect of molybdenum and chromium contents in sliding wear of high-chromium white cast iron: The relationship between microstructure and wear, Wear **267** (2009) 401–408.

[43] A. Bedolla-Jacuinde, W.M. Rainforth, The wear behaviour of high-chromium white cast irons as a function of silicon and mischmetal content, Wear **250** (2001) 449––461.

[44] K. Peev, M. Radulovic, M. Fiset, Modification of Fe-Cr-C alloys using mischmetal, J. Mater. Sci. Lett. 13 (1994) 112–114.

[45] M. Radulovic, M. Fiset, K. Peev, Effect of rare earth elements on microstructure and properties of high chromium white iron, Mater. Sci. Technol. **10** (1994) 1057––1062.

[46] Y. Qu, J. Xing, X. Zhi, J. Peng, H. Fu, Effect of cerium on the as-cast microstructure of a hypereutectic high chromium cast iron, Mater. Mater. Lett. **62** (2008) 3024––3027.

[47] P. Dupin, J.M. Schissler, Influence of additions of silicon, molybdenum, vanadium, and tungsten upon the structural evolution of the as-cast state of a high-chromium cast iron (20%Cr, 2.6%C), AFS Trans. **92** (1984) 355–360.

[48] Y. Matsubara, N. Sasaguri, K. Shimizu, S.K. Yu, Solidification and abrasion wear of white cast irons alloyed with 20% carbide forming elements, Wear **250** (2001) 502–510.

[49] D.M. Stefanescu, S. Cracium, Manganese and vanadium cast iron with 15% chromium for abrasive wear resistant castings, Fonderie **32** (1977) 51–60.

[50] A. Bedolla-Jacuinde, B. Hernández, L. Béjar-Gómez, SEM study on the M_7C_3 carbide nucleation during eutectic solidification of high-chromium white irons, Z. Metallkd. **96** (2005) 1380–1385.

[51] W. Kurz, D.J. Fisher, Fundamentals of Solidification, Trans Tech Publication, Dürnten, 1984, pp. 97–116.

[52] M. Asta, C. Beckermann, A. Karma, W. Kurz, R. Napolitano, M. Plapp, G. Purdy, M. Rappaz, R. Trivedi, Solidification microstructures and solid-state parallels: Recent developments, future directions, Acta Mater. **57** (2009) 941–971.

[53] S.D. Carpenter, D. Carpenter, J.D.H. Pearce, XRD and electron microscope study of an as-cast 26.6% chromium white iron microstructure, Mater. Chem. and Phys. **85** (2004) 32–40.

[54] Ö.N. Doğan, J.A. Hawk, G. Laird II, Solidification structure and abrasion resistance of high chromium white irons, Met. Mat. Trans., A **28** (1997) 1315–1328.

[55] K. Ogi, Y. Matsubara, K. Matsuda, Eutectic solidification of high chromium cast iron — mechanism of eutectic growth, AFS Trans. **89** (1981) 197–204.

[56] X. Zhi, J. Xing, Y. Gao, H. Fu, J. Peng, B. Xiao, Effect of heat treatment on microstructure and mechanical

properties of a Ti-bearing hypereutectic high chromium white cast iron, Mater. Sci. Eng., A **487** (2008) 171–179.

[57] R.S.J. Jackson, The austenite liquidus surface and constitutional diagram for the Fe–Cr–C metastable system, Iron Steel Inst. **208** (1970) 163–167.

[58] L. Lu, H. Soda, A. McLean, Microstructure and mechanical properties of Fe–Cr–C eutectic composites, Mater. Sci. Eng., A **347** (2003) 214–222.

[59] H. Liu, J. Wang, H. Yang, B. Shen, Effects of cryogenic treatment on microstructure and abrasion resistance of CrMnB high chromium cast iron subjected to sub-critical treatment, Mater. Sci. Eng., A **478** (2008) 324–328.

[60] J. Wang, J. Xiong, H. Fan, H.S. Yang, H.H. Liu, B.L. Shen, Effects of high temperature and cryogenic treatment on the microstructure and abrasion resistance of a high chromium cast iron, J. Mater. Process. Technol. **209** (2009) 3236–3240.

[61] I. Karaman, H. Sehitoglu, Y.I. Chumlyakov, H.J. Maier, The deformation of low-stacking-fault-energy austenitic steels, JOM **54** (2002) 31–37.

IZVOD

ŽELEZO-HROM-UGLJENIK-VANADIJUM BELA LIVENA GVOŽĐA – MIKROSTRUKTURA I SVOJSTVA

Mirjana M. Filipović

Tehnološko-metalurški fakultet, Univerzitet u Beogradu, Beograd, Srbija

(Pregledni rad)

Mikrostruktura Fe–Cr–C–V belih gvožđa u livenom stanju se sastoji od M_7C_3 karbida i M_6C_5 karbida bogatih vanadijumom u austenitnoj metalnoj osnovi. Vanadijum menja mikrostrukturne parametre faza prisutnih u strukturi ovih legura, uključujući zapreminski udeo, veličinu i morfologiju. Stepen martenzitne transformacije, takođe, zavisi od sadržaja vanadijuma u leguri. Zapreminski udeo karbidne faze, veličina karbida i raspodela ima značajan uticaj na otpornost na habanje abrazijom Fe–Cr–C–V belih livenih gvožđa u uslovima malih naprezanja. Međutim, žilavost Fe–Cr–C–V gvožđa je uglavnom određena svojstvima metalne osnove. Austenit je mnogo efektniji od martenzita. Budući da austenit u ovim legurama sadrži vrlo fine čestice $M_{23}C_6$ karbida, veća žilavost je povezana sa ojačavanjem austenita u toku loma. Pored toga, sekundarni karbidi, istaloženi u regionima metalne osnove, takođe, utiču na ponašanje pri habanju abrazijom. Povećavajući čvrstoću metalne osnove kroz efekat disperznog ojačavanja, fini sekundarni karbidi povećavaju mehaničku podršku eutektičkim karbidima. U uslovima ponovljenih udarnih opterećenja u zaostalom austenitu Fe–Cr–C–V belih gvožđa javlja se deformacija i deformaciono ojačavanje. Čestice istaloženih $M_{23}C_6$ sekundarnih karbida ometaju kretanje dislokacija i doprinose pojačanju efekta deformacionog ojačavanja.

Ključne reči: Fe–Cr–C–V bela livena gvožđa • Mikrostruktura • Tvrdoća • Žilavost • Otpornost na habanje abrazijom • Otpornost na ponovljena udarna opterećenja